Tectonics®

RESEARCH ARTICLE
10.1029/2025TC009001

Key Points:

- Fault throw-rate scatter increases with more closely spaced faults across strike in extensional regions
- Stronger throw-rate versus fault length correlation occurs where fewer faults interact across strike
- Evaluation of throw rate scatter is important for seismic hazard analysis

Supporting Information:

Supporting Information may be found in the online version of this article.

Correspondence to:

M. Meschis,
marco.meschis@ingv.it

Citation:

Meschis, M., Mildon, Z. K., Roberts, G. P., Sgambato, C., Livio, F., Michetti, A. M., et al. (2026). Empirical scaling relationships between fault length and throw-rates modulated by fault interactions in extensional regimes. *Tectonics*, *45*, e2025TC009001. https://doi.org/10.1029/2025TC009001

Received 15 MAY 2025
Accepted 23 APR 2026

Author Contributions:

Conceptualization: M. Meschis, Z. K. Mildon, G. P. Roberts
Data curation: M. Meschis, Z. K. Mildon, G. P. Roberts, C. Sgambato, J. Faure Walker
Formal analysis: M. Meschis, F. Livio, J. Faure Walker
Funding acquisition: A. Gattuso, A. Caracausi
Investigation: M. Meschis, Z. K. Mildon, G. P. Roberts, C. Sgambato, A. M. Michetti, J. Robertson
Methodology: M. Meschis, G. P. Roberts, F. Livio, A. M. Michetti, J. Faure Walker
Project administration: A. Caracausi
Validation: M. Meschis, Z. K. Mildon, G. P. Roberts, A. M. Michetti, J. Robertson, J. Faure Walker, F. Iezzi
Visualization: M. Meschis, G. P. Roberts, F. Livio

Empirical Scaling Relationships Between Fault Length and Throw-Rates Modulated by Fault Interactions in Extensional Regimes

M. Meschis[1], Z. K. Mildon[2], G. P. Roberts[3], C. Sgambato[3], F. Livio[4], A. M. Michetti[4,5], J. Robertson[3], J. Faure Walker[6], F. Iezzi[7], A. Gattuso[1], M. D. Barberio[8], P. Randazzo[1], and A. Caracausi[1]

[1]Istituto Nazionale di Geofisica e Vulcanologia (INGV), Sezione Palermo, Palermo, Italy, [2]School of Geography, Earth and Environmental Sciences, University of Plymouth, Plymouth, UK, [3]School of Natural Sciences, Birkbeck, University of London, London, UK, [4]Università degli Studi dell'Insubria, Como, Italy, [5]Istituto Nazionale di Geofisica e Vulcanologia (INGV), Sezione Osservatorio Vesuviano, Italy, [6]Department of Risk and Disaster Reduction, University College London, London, UK, [7]DISTAR - Department of Earth, Environmental and Resources Sciences, University of Naples Federico II, Italy, [8]Istituto Nazionale di Geofisica e Vulcanologia (INGV), Sezione Roma 1, Italy

Abstract

Throw rates of active faults are expected to scale with fault length because the geometric moment of a fault is directly related to its dimensions. However, empirical data sets commonly display substantial scatter, which limits the use of fault scaling relationships for seismic hazard assessment and for understanding the mechanics of continental deformation. Here we compile and investigate throw-rate versus fault-length data sets from three extensional regions in Italy characterized by progressively increasing numbers of active faults across strike. For each region, we quantify the strength and scatter of the scaling relationship using multiple statistical metrics, including R^2, RMSE, and SSE. Our results show that the strength of the correlation systematically decreases and scatter increases as the number of across-strike faults increases. This pattern is robust across statistical measures and is not significantly affected by uncertainties in fault length or throw-rate estimation over Holocene to Late Quaternary timescales. We interpret these observations as evidence that fault interaction within densely faulted systems plays a first-order role in controlling throw-rate variability. These findings have important implications for the application of fault scaling relationships to seismic hazard assessment and for models of strain partitioning in continental extensional settings.

Plain Language Summary

This study investigates the variability in empirical scaling relationships between fault throw-rate and fault length across extensional regions of the Italian Apennines. While longer faults are generally expected to have higher slip rates, significant scatter in observed data complicates seismic hazard assessments. By analyzing data sets from three regions with differing fault network geometries within the Italian Apennines Chain, the authors demonstrate that the degree of scatter correlates with the number of faults across strike. Regions with more faults in close proximity show greater variability in throw-rate versus length, attributed to fault interactions that modulate slip rates through stress change transfer processes. These findings align with previous hypotheses that temporal earthquake clustering and variable slip rates arise from fault network interactions. The results underscore the importance of considering fault geometry, particularly across-strike spacing, when using scaling laws for seismic hazard modeling or estimating crustal rheology. The study suggests that more accurate seismic hazard assessments can be achieved by accounting for fault interaction effects, especially in densely faulted regions where stress change transfer from one fault can significantly impact the behavior of neighboring structures.

1. Introduction

Fault displacement-rates, whether reported as slip in the plane of the faults (slip-rates) or throw-rates (vertical component of the slip-rate), are critical variables used for seismic hazard assessment because they influence the recurrence rates of earthquakes (Cowie & Roberts, 2001; Cowie et al., 2012; Molnar, 1979; Nicol et al., 2005; Pace et al., 2016; Sgambato, Faure Walker, & Roberts, 2020). For instance, such data from active faults are currently used in probabilistic seismic hazard assessment (PSHA) to assess the associated seismic hazard (e.g., Field et al., 2014; Pace et al., 2006; Peruzza et al., 2011; A. Valentini et al., 2017). Average earthquake recurrence intervals tend to decrease as throw-rates increase (e.g., Cowie & Roberts, 2001; Wesnousky, 1999),

Writing – original draft: M. Meschis
Writing – review & editing: Z. K. Mildon, G. P. Roberts, C. Sgambato, F. Livio, A. M. Michetti, J. Robertson, J. Faure Walker, F. Iezzi, A. Gattuso, M. D. Barberio, P. Randazzo, A. Caracausi

but unfortunately throw-rates may not be available for some faults in a region. Indeed, lack of knowledge for fault throw-rates might be due for several reasons such as slow fault movement, complex fault geometries, limited or inaccessible field measurements, erosion or sedimentation obscuring geological markers and lack of suitable materials for geochronological dating (e.g., Gómez-Novell et al., 2022). One approach to estimating slip/throw-rates, where their direct measurements are lacking, is to exploit scaling relationships between throw-rates and fault length, because the latter is amenable to measurement from surface mapping. The slip-rates of faults are expected to scale with the fault lengths because the geometric moment (Mg) for a given fault, is related to the fault displacement (D), the length of the fault (L) and the down-dip width (W), in the form $Mg = DLW$ (e.g., Anderson et al., 2021; Cowie & Roberts, 2001; Scholz & Cowie, 1990; Wells & Coppersmith, 1994; Wesnousky, 1999, 2008). However, significant scatter exists in data sets for this relationship, and lack of understanding of why the scatter exists hinders our ability to use it for seismic hazard purposes and to understand continental deformation (Mouslopoulou et al., 2009). One suggestion is that the scatter is introduced where temporal earthquake clustering raises or lowers the throw-rate measured over timescales of a few millennia relative to time-averaged throw-rates measured over tens to hundreds of millennia or more (Mouslopoulou et al., 2009). Indeed, in Mouslopoulou et al. (2009), the temporal earthquake clustering was suggested to be produced by fault interactions, but data available to test this was not discussed in detail. Since that time several studies have detailed throw-rate variability and temporal earthquake clustering associated with fault interactions (e.g., Iezzi et al., 2021; Roberts et al., 2024, 2025). For example, for areas of extensional faulting in Italy, it has been shown that the transfer of stress produced by coseismic and interseismic slip is of sufficient magnitude to modulate the strain-rates on viscous shear-zones underlying active normal faults to an extent that explains the measured throw-rate variations on their overlying faults (e.g., Mildon et al., 2022; Roberts et al., 2024, 2025). These studies showed that throw-rates within 42 studied temporal earthquake clusters, lasting on average between 2.83 and 4.26 kyrs, are greater than throw-rate measured over 20 kyrs by a mean factor of 6.24 (Roberts et al., 2025). This is consistent with the hypothesis advanced by Mouslopoulou et al. (2009).

Previous investigations have interpreted fault network geometry, and in particular the number and across-strike spacing of active faults, as exerting a first-order control on fault interaction processes (e.g., Roberts et al., 2024; Rodriguez Piceda et al., 2025). In extensional regions where multiple active faults are closely spaced across strike, coseismic and interseismic stress changes produced by slip on individual faults may be more efficiently transferred to neighboring structures, promoting temporal variability in slip rates and increasing the likelihood of earthquake clustering within fault systems (e.g., Cowie et al., 2012; Gupta & Scholz, 2000; Nicol et al., 2005). For instance, the importance of fault network geometry, particularly the across-strike and along-strike proximity of faults, in controlling stress evolution has been demonstrated by Sgambato et al., 2023. Indeed, in this study has been highlighted how fault geometry affects the relative importance of coseismic and interseismic stresses, and consequently the proportion of faults that are positively stressed over time. Furthermore, they showed how the stress evolution associated with earthquake recurrence differs in three regions of extension along the Italian Apennines such as the Central Apennines, the Southern Apennines and Calabria and the Messina Strait region which have a differing fault network geometry, including the number of faults across-strike which accommodate the extension. However, it remains poorly quantified whether fault network geometry systematically controls the scatter of long-term throw-rate versus fault-length scaling relationships. These results prompted us to test the hypothesis that greater scatter in throw-rate versus fault length scaling will exist for faults systems with geometries that promote interaction, for example, where a greater number of faults exist across strike, and the separation of faults across strike is small relative to the distance across strike that significant stress interactions can occur. We present throw-rate versus fault length data sets for three areas of extension in Italy that exhibit a progressively greater number of closely spaced faults across strike. We show that the scatter in the data increases with a greater number of faults across strike and hence greater across strike fault interaction. We discuss these results in terms of seismic hazard assessment and continental deformation.

2. Geological Background and Regional Setting

This study focuses on three regions within the extensional Italian Apennines Chain (Figure 1 and inset): the Central Apennines, the Southern Apennines, and Calabria and the Messina Strait region, which have varying fault network geometry, in particular the number of faults across-strike which accommodate the extension.

10.1029/2025TC009001

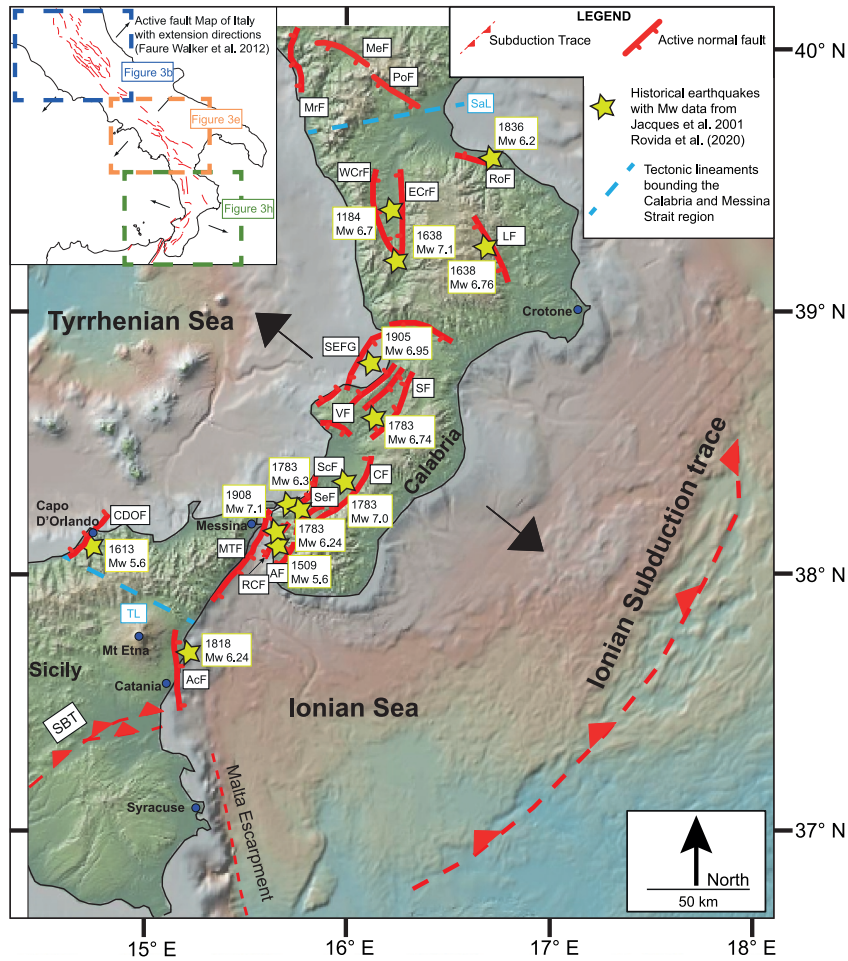

Figure 1. Map showing active normal faults deforming the Calabria and Messina Strait region in the southern Italian Apennines chain. Yellow stars represent location of historical earthquakes with highest magnitude for a given fault. In dashed and light-blue colored lines tectonic lineaments are shown, identifying the north and south limits of the Calabria and Messina Strait region. Top inset is modified from Faure Walker et al. (2012).

2.1. Extension in the Italian Apennines Chain

The Italian Apennines Chain is formed by previously shortened continental crust produced by the Alpine orogenesis, lying within a zone of tectonic convergence between African and Eurasian Plates, later affected by active extension since Plio-Pleistocene times (Cavinato & Celles, 1999; Doglioni, 1993; Malinverno & Ryan, 1986). Crustal extension is thought to be likely due to a combined process between (a) the roll-back of the Calabrian subduction zone and (b) mantle upwelling beneath the continental crust (Cavinato & Celles, 1999; D'Agostino et al., 2001; Faure Walker et al., 2012; Gvirtzman & Nur, 1999, 2001; Malinverno & Ryan, 1986). In particular, in the Central and Southern Apennines, southwest–northeast extension initiated at ∼2–3 Ma and is accommodated by arrays of NW–SE–striking normal faults that are commonly segmented and intersected by across-strike structures (Cavinato & Celles, 1999; Patacca & Scandone, 2007; Roberts & Michetti, 2004). Surface fault scarps preserved since the Last Glacial Maximum (∼15 ± 3 ka) record cumulative surface-rupturing earthquakes, providing robust estimates of post-glacial throw-rates that are broadly representative of longer-term deformation since fault initiation at ∼1.8–3.0 Ma (Faure Walker et al., 2012; Papanikolaou & Roberts, 2007). This structurally complex fault network promotes strong fault interactions and spatially variable slip, making the Apennines an ideal setting for investigating throw-rate variability and temporal clustering. In contrast, the Calabrian-Peloritan Arc forms a transitional zone between the Southern Apennines and the Maghrebian chain of northern Sicily and is dominated by Quaternary WNW–ESE extension associated with the southeastward retreat of the Ionian slab (e.g., Faccenna et al., 2001). Deformation is accommodated by fewer, longer-lived

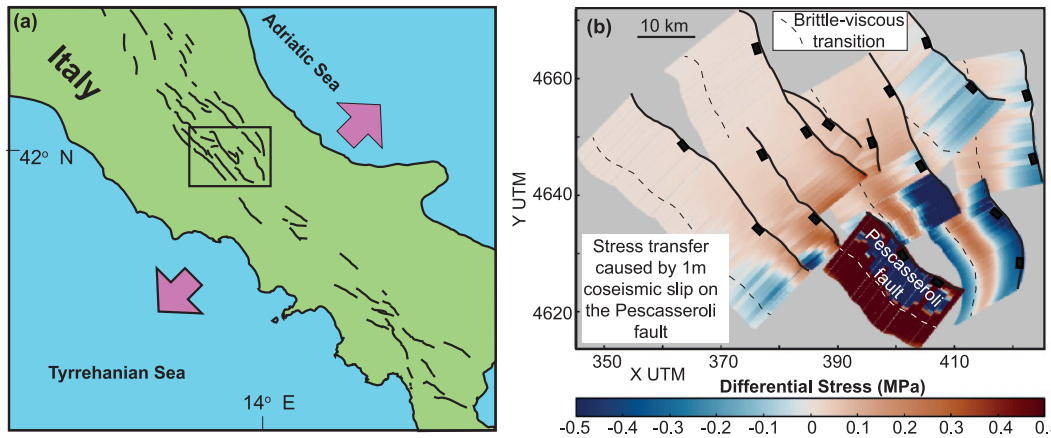

Figure 2. Stress transfer across a system of faults resulting from a 1 m coseismic slip event on an active normal fault. Significant stress changes occur across a region contain multiple faults across strike. Modified from Roberts et al. (2024).

normal faults, many of which have accumulated substantial throw since the Middle Pleistocene (~0.7 Ma) and are associated with prominent fault scarps and uplifted marine terraces (e.g., Monaco & Tortorici, 2000; Quye-Sawyer et al., 2021; Roberts et al., 2013). Slip or throw rates derived from displaced Holocene deposits and Quaternary terraces are relatively well constrained and are consistent with high geodetic strain rates measured across the region (Devoti et al., 2011; Meschis, Teza, et al., 2022). Compared to the Apennines, the Calabrian-Sicily fault network is characterized by wider fault spacing and fewer across-strike structures, representing a geometrically simpler end-member. This contrast between a highly segmented fault system (Apennines) and a more linear, along-strike fault network (Calabria-Sicily) provides a natural framework for testing how fault-network geometry influences throw-rate variability, fault interaction, and the temporal clustering of large earthquakes.

Crustal extension that has affected the uplifting Italian Apennines Chain, accommodated by active normal faults, is consistent with GNSS measurements showing an averaged extension rate within a range of ~2–3 mm/yr (Faure Walker et al., 2012; Mastrolembo Ventura et al., 2014; Meschis, Roberts, et al., 2022; Meschis, Teza, et al., 2022; Serpelloni et al., 2005; Walker, 2010). Active extension is also confirmed by the presence of historical seismic activity in the last millennia that have ruptured these normal faults along the Italian Apennines Chain throughout Calabria and the Messina Strait region (e.g., Aloisi et al., 2013; Galli et al., 2007; Giuffrida et al., 2023; Jacques et al., 2001; Meschis et al., 2019). Roberts et al. (2024) showed that stress transfer from a single 1-m coseismic slip event produces differential stress changes in the range of ±0.1 to >0.5 MPa on faults across the whole width of the Apennines normal fault system, and on shear-zones beneath these active faults (Figure 2). With stress changes experienced over across strike distances of ~60 km, and average across-strike fault spacings of 8–15 km, it appears that the separation of faults across strike is small relative to the distance across strike that significant stress interactions can occur.

3. Methods and Details of Fault Data for the Italian Apennines Chain

For this study we compiled data for 68 active normal faults as summarized in Table 1 where fault lengths and fault throw-rates are shown for the Central Apennines, Southern Apennines and Calabria and Messina Strait region (Sicily). All fault throw-rates data from the literature are stated using the largest measured value along a fault trace. For the Calabria and Messina Strait region almost all fault throw-rates are averaged over the Middle to Late Pleistocene (700–15 ka) because they are derived by displaced and tectonically-deformed raised marine terraces (e.g., Ferranti et al., 2006; Meschis et al., 2018; Meschis, Roberts, et al., 2022; Meschis, Teza, et al., 2022; Roberts et al., 2013; Roda-Boluda & Whittaker, 2017; Westaway, 1993). These time periods are long relative to the 2.83–4.26 kyrs temporal extents of temporal earthquake clusters measured elsewhere in the Apennines (Mildon et al., 2022; Roberts et al., 2024, 2025). In contrast, fault throw-rates from the Southern Apennines and Central Apennines regions are mostly values averaged since the demise of the Last Glacial Maximum (LGM) at ~15 ± 3 ka, but also derived from raised and displaced Holocene coastal notches studies, and Holocene

Table 1
Fault Data Are Shown

Fault	Length—L (km)	Throw rate—TR (mm/yr)	Time spanning for throw-rates	Reference
Calabria and Messina Strait region				
Rossano	15	0.47	125 ka*	Galli et al. (2011)
East Crati	45	1.3	700 ka*	Roda-Boluda and Whittaker (2017)
West Crati	40	0.8	700 ka*	Roda-Boluda and Whittaker (2017), Meschis, Teza, et al. (2022), Tortorici et al. (1995)
Lakes	33	1.08	15 ka?	Galli et al. (2007), Galli and Bosi (2003)
Sant'Eufemia Gulf	24	0.21	15 ka?	Loreto et al. (2023), A. Valentini et al. (2017)
Vibo	24	1.06	340 ka*	Roberts et al. (2013)
Serre	32	0.8	600 ka*	Roda-Boluda and Whittaker (2017)
Cittanova	47	1.4	600 ka*	Roda-Boluda and Whittaker (2017)
Scilla	30	0.95	15 ka?	Ferranti et al. (2007, 2008)
Sant'Eufemia	19	0.86	700 ka*	A. Valentini et al. (2017), Monaco and Tortorici (2007)
Armo	18	0.32	50 ka*	Meschis, Roberts, et al. (2022)
Reggio Calabria	20	0.33	50 ka*	Meschis, Roberts, et al. (2022)
Messina-Taormina	58	2.34	50 ka*	Meschis, Roberts, et al. (2022), Meschis et al. (2019)
Capo D'Orlando	22	0.63	340 ka*	Meschis et al. (2018)
Southern Apennines				
Alburni	24	0.43	15 ka	Sgambato, Faure Walker, and Roberts (2020), Sgambato, Faure Walker, Mildon, and Roberts (2020)
Apice	6	0.20	15 ka	Sgambato, Faure Walker, and Roberts (2020), Sgambato, Faure Walker, Mildon, and Roberts (2020)
Avella	20	0.20	15 ka	Sgambato, Faure Walker, and Roberts (2020), Sgambato, Faure Walker, Mildon, and Roberts (2020)
Boiano	26	0.44	15 ka	Sgambato, Faure Walker, and Roberts (2020), Sgambato, Faure Walker, Mildon, and Roberts (2020)
Cassino	24	0.40	15 ka	Sgambato, Faure Walker, and Roberts (2020), Sgambato, Faure Walker, Mildon, and Roberts (2020)
Gallo	13.5	0.20	15 ka	Sgambato, Faure Walker, and Roberts (2020), Sgambato, Faure Walker, Mildon, and Roberts (2020)
Irpinia	26	0.65	15 ka	Sgambato, Faure Walker, and Roberts (2020), Sgambato, Faure Walker, Mildon, and Roberts (2020)
Irpinia Antithetic	8	0.33	15 ka	Sgambato, Faure Walker, and Roberts (2020), Sgambato, Faure Walker, Mildon, and Roberts (2020)
Maratea	23	0.52	15 ka	Sgambato, Faure Walker, and Roberts (2020), Sgambato, Faure Walker, Mildon, and Roberts (2020)
Mercure	24	0.45	15 ka	Sgambato, Faure Walker, and Roberts (2020), Sgambato, Faure Walker, Mildon, and Roberts (2020)
Miranda Pesche	8.5	0.20	15 ka	Sgambato, Faure Walker, and Roberts (2020), Sgambato, Faure Walker, Mildon, and Roberts (2020)
Monte Alpi	20	0.60	15 ka	Sgambato, Faure Walker, and Roberts (2020), Sgambato, Faure Walker, Mildon, and Roberts (2020)
Piedimonte Matese	11	0.20	15 ka	Sgambato, Faure Walker, and Roberts (2020), Sgambato, Faure Walker, Mildon, and Roberts (2020)
Pollino	25	0.40	15 ka	Sgambato, Faure Walker, and Roberts (2020), Sgambato, Faure Walker, Mildon, and Roberts (2020)

Table 1
Continued

Fault	Length—L (km)	Throw rate—TR (mm/yr)	Time spanning for throw-rates	Reference
Pozzilli	17	0.22	15 ka	Sgambato, Faure Walker, and Roberts (2020), Sgambato, Faure Walker, Mildon, and Roberts (2020)
San Gregorio Magno	23	0.51	15 ka	Sgambato, Faure Walker, and Roberts (2020), Sgambato, Faure Walker, Mildon, and Roberts (2020)
Ufita	13	0.20	15 ka	Sgambato, Faure Walker, and Roberts (2020), Sgambato, Faure Walker, Mildon, and Roberts (2020)
Val d'Agri	36	0.61	15 ka	Sgambato, Faure Walker, and Roberts (2020), Sgambato, Faure Walker, Mildon, and Roberts (2020)
Vallo di Diano	39	0.67	15 ka	Sgambato, Faure Walker, and Roberts (2020), Sgambato, Faure Walker, Mildon, and Roberts (2020)
Volturara	23.5	0.30	15 ka	Sgambato, Faure Walker, and Roberts (2020), Sgambato, Faure Walker, Mildon, and Roberts (2020)
Volturno	15.5	0.50	15 ka	Sgambato, Faure Walker, and Roberts (2020), Sgambato, Faure Walker, Mildon, and Roberts (2020)
Ufita	13	0.20	15 ka	Sgambato, Faure Walker, and Roberts (2020), Sgambato, Faure Walker, Mildon, and Roberts (2020)
Val d'Agri	36	0.61	15 ka	Sgambato, Faure Walker, and Roberts (2020), Sgambato, Faure Walker, Mildon, and Roberts (2020)
Vallo di Diano	39	0.67	15 ka	Sgambato, Faure Walker, and Roberts (2020), Sgambato, Faure Walker, Mildon, and Roberts (2020)
Volturara	23.5	0.30	15 ka	Sgambato, Faure Walker, and Roberts (2020), Sgambato, Faure Walker, Mildon, and Roberts (2020)
Volturno	15.5	0.50	15 ka	Sgambato, Faure Walker, and Roberts (2020), Sgambato, Faure Walker, Mildon, and Roberts (2020)
Central Apennines				
Assergi	25	0.84	15 ka	Faure Walker et al. (2021)
Barete	16	0.76	15 ka	Faure Walker et al. (2021)
Barisciano	22	0.46	15 ka	Faure Walker et al. (2021)
Barisciano Mt. Stabiata	37	0.46	15 ka	Faure Walker et al. (2021)
Campo Felice	11	0.96	15 ka	Faure Walker et al. (2021)
Campo Imperatore East	21	0.45	15 ka	Faure Walker et al. (2021)
Carsoli	19	0.47	15 ka	Faure Walker et al. (2021)
Cerchio Pescina Parasano	18	0.64	15 ka	Faure Walker et al. (2021)
Cinque Miglia Aremogna	18	0.77	15 ka	Faure Walker et al. (2021)
Frattura	17	0.84	15 ka	Faure Walker et al. (2021)
Fucino Magnola	37	1	15 ka	Faure Walker et al. (2021)
Fucino Ovindoli Pezza	41	1.56	15 ka	Faure Walker et al. (2021)
Laga	33	0.65	15 ka	Faure Walker et al. (2021)
Leonessa	19	0.43	15 ka	Faure Walker et al. (2021)
Liri	47	1.33	15 ka	Faure Walker et al. (2021)
Magnola	10	0.45	15 ka	Faure Walker et al. (2021)
Maiella	25	0.83	15 ka	Faure Walker et al. (2021)
Middle Aterno Valley	20	0.57	15 ka	Faure Walker et al. (2021)
Mt. Marsicano	24	0.66	15 ka	Faure Walker et al. (2021)
Mt. Pizzalto	8	0.20	15 ka	Faure Walker et al. (2021)

Table 1
Continued

Fault	Length—L (km)	Throw rate—TR (mm/yr)	Time spanning for throw-rates	Reference
Mt. Velino	25	0.56	15 ka	Faure Walker et al. (2021)
Mt. Vettore	38	1.66	15 ka	Faure Walker et al. (2021)
Norcia	24	0.66	15 ka	Faure Walker et al. (2021)
Ocre	7	0.42	15 ka	Faure Walker et al. (2021)
Ovindoli Pezza	17	1.56	15 ka	Faure Walker et al. (2021)
Paganica.SanDemetrio Mt. Stabiata	24	0.46	15 ka	Faure Walker et al. (2021)
Paganica SanDemetrio NeVestini	17	0.3	15 ka	Faure Walker et al. (2021)
Rieti	22	0.33	15 ka	Faure Walker et al. (2021)
San Sebastiano	14	0.33	15 ka	Faure Walker et al. (2021)
Scanno	33	0.84	15 ka	Faure Walker et al. (2021)
Scurcola	35	1	15 ka	Faure Walker et al. (2021)
Sella Di Corno	25	0.4	15 ka	Faure Walker et al. (2021)
Sulmona	26	1.33	15 ka	Faure Walker et al. (2021)

Note. Fault slip-rates are spanning the Holocene but "starred" value data (all from Calabria and Messina Strait region) are spanning the Middle to Late Pleistocene.

palaeoseismological data and displaced fault scarps investigations as reported previously (Faure Walker et al., 2021 and reference therein and in Table 1). Again, we note that these time periods are long relative to the temporal extents of temporal earthquake clusters measured elsewhere in the Apennines. Indeed, these timescales used in this study exceed the duration of documented temporal earthquake clustering and therefore represent long-term fault behavior rather than short-term transient variability.

We emphasize once again that we assume stability in the fault throw rates during the Quaternary. Throw-rates calculated over the last 15 ka do not differ substantially from those calculated over 700 ka. This seems like a reasonable assumption, even if we know that there are fluctuations, and that in reality the extensional tectonics in Italy has progressively decreased in intensity over the last million years (e.g., Carminati et al., 2010). Fault lengths and fault throw-rates for the Calabria and Messina Strait region have been compiled for this study from literature (Table 1 and Figure 1). Data on fault lengths and throw-rates for the other two tectonically-extending regions of Italian Apennines are from the literature (Faure Walker et al., 2021; Mildon, Roberts, Faure Walker, Beck, et al., 2019; Mildon, Roberts, Faure Walker, & Toda, 2019; Sgambato, Faure Walker, Mildon, & Roberts, 2020; Sgambato, Faure Walker, & Roberts, 2020). It is important to note that fault lengths used in this study are taken from well-accepted fault maps and databases properly cited in Table 1 and correspond to mapped surface traces of individual active faults. Moreover, these definitions are applied in a consistent way across all the three investigated regions in this study. We are aware that one can argue that adjacent fault segments may be mechanically linked at depth (i.e., soft linkage, Faure Walker et al., 2009; Iezzi et al., 2019; Rotevatn et al., 2019), yet we do not modify published fault lengths as doing so would introduce regionally variable assumptions and reduce internal consistency. Furthermore, independent investigations have proved that fault lengths available from literature are reliable and scaled with magnitudes of historical and paleoseismologically-derived seismic events (Galli et al., 2008; Schirripa Spagnolo et al., 2021). We know of places where fault maps and lengths are not well defined, however we argue that accepting the uncertainty will not dramatically affect our results. To this end, we have also applied margin of errors of 10% for fault length and 20% for fault throw-rates (Walker, 2010).

For our statistical analysis, we explored the linear regression between throw-rate (TR) and fault length (L), adopting the following equation:

$$TR = a * L + b$$

Where a and b are regression parameters fitted via a least squares best fit analysis. The 95% confidence bounds of the regressed parameters are reported, as well. Goodness of fit is evaluated through the SSE (Sum of Squares due to Error), R^2, and RMSE (Root Mean Squared Error). SSE is the total squared deviation of observed from predictive values; it represents the total prediction error made by the model across all observations and it is also the quantity that ordinary least squares approach explicitly minimizes during the fitting process. Note that it is not directly comparable between data sets of different sizes. RMSE measures the magnitude of the residuals in the units of the dependent variable (mm/yr), providing an intuitive measure of scatter around the regression: it is not dependent on the size of the sample, but it is more sensitive to possible outliers.

Finally, R^2 value (coefficient of determination) quantifies in this study the proportion of variance in throw rates that is explained by fault length; indeed, a value of 1 indicates perfect prediction and 0 indicates no explanatory power.

The adoption of a linear regression between TR and L is theoretically suggested by fracture-mechanics that predicts self-similar growth (Cowie & Scholz, 1992), which, over certain stages of fault evolution or regional fault sampling, can produce an approximately linear TR–L regression.

It is important to note that where deformation rates are stated in the literature as slip-rate we converted values to throw-rates, which is the vertical component of the displacement rate, using values for fault dip gathered from surface outcrops in the literature.

In order to facilitate comparison with data set by Mouslopoulou et al. (2009), we have normalized our throw-rates data to that for a notional 100 km long fault in each of the three areas to remove the effect of differing regional extension rates along the strike of the Apennines Chain. In particular, in order to allow comparison between data sets spanning different absolute ranges of fault length and throw rate, we have normalized fault length and throw rate following the approach of Mouslopoulou et al. (2009). Specifically, fault throw rates were scaled to a reference fault length of 100 km by normalizing individual fault lengths (L) to 100 km and adjusting throw rates accordingly. The choice of a 100-km reference length reflects the upper bound of fault lengths commonly observed for mature continental normal faults and provides a physically meaningful scale for inter-regional comparison. This normalization preserves the internal scaling and relative scatter within each data set while removing first-order differences in absolute magnitude related to regional strain rates and tectonic setting.

Finally, we sampled the numbers of faults across strike in each area via serial linear transects parallel to the extension direction and compiled this information using histograms and producing frequency distributions (Figure 3), to highlight the variations in fault network geometry along the Apennine chain.

4. Results

In this section, we show our new refined empirical correlations between fault length and fault throw-rates for each investigated region such as the Central Apennines, Southern Apennines, and Calabria and Sicily. In particular, Figures 3a–3i shows the results for each of the three areas. The regressions calculated in all the considered regions show a positive value for the parameter a (slope of the regression), whereas the 95% bounds for the b parameter (intercept) cross the zero (Table 2). Calabria-Sicily data set shows the strongest correlation ($R^2 = 0.72$; Figure 3g), indicating that approximately 72% of the variability in throw rate is explained by fault length alone in this region. This is in contrast with the Central Apennines ($R^2 = 0.34$; Figure 3a), where only 34% of the throw rate variance is justified by fault length, suggesting that other controlling factors, including fault interaction, may exert a prominent influence. The Southern Apennines shows an intermediate value ($R^2 = 0.55$; Figure 3d). SSE values decrease systematically from the Central Apennines to Calabria-Sicily, consistent with the improvement of R^2, even if we note that SSE is sensitive to sample size and should not be compared directly between regions of different fault count (Table 2). Instead, RMSE values are lowest for the Southern Apennines (Figure 3d), indicating that the typical residual in throw rate around the regression line is smallest in that region; the Central Apennines and Calabria-Sicily data sets show higher, comparable RMSE values. We show that, taken together, these metrics indicate that differences between regions are robust and do not depend on a single statistical indicator. It is important to highlight that fitting metrics measure the proportion of explained variance, not the sensitivity of throw rate to length nor any bias direction (i.e., over/under-prediction). For example, a high R^2 and a low RMSE do not preclude a shallow regression gradient (i.e., throw rate may not vary greatly across the range of fault lengths observed). In this line, it is therefore important to note that the gradient of the linear regression

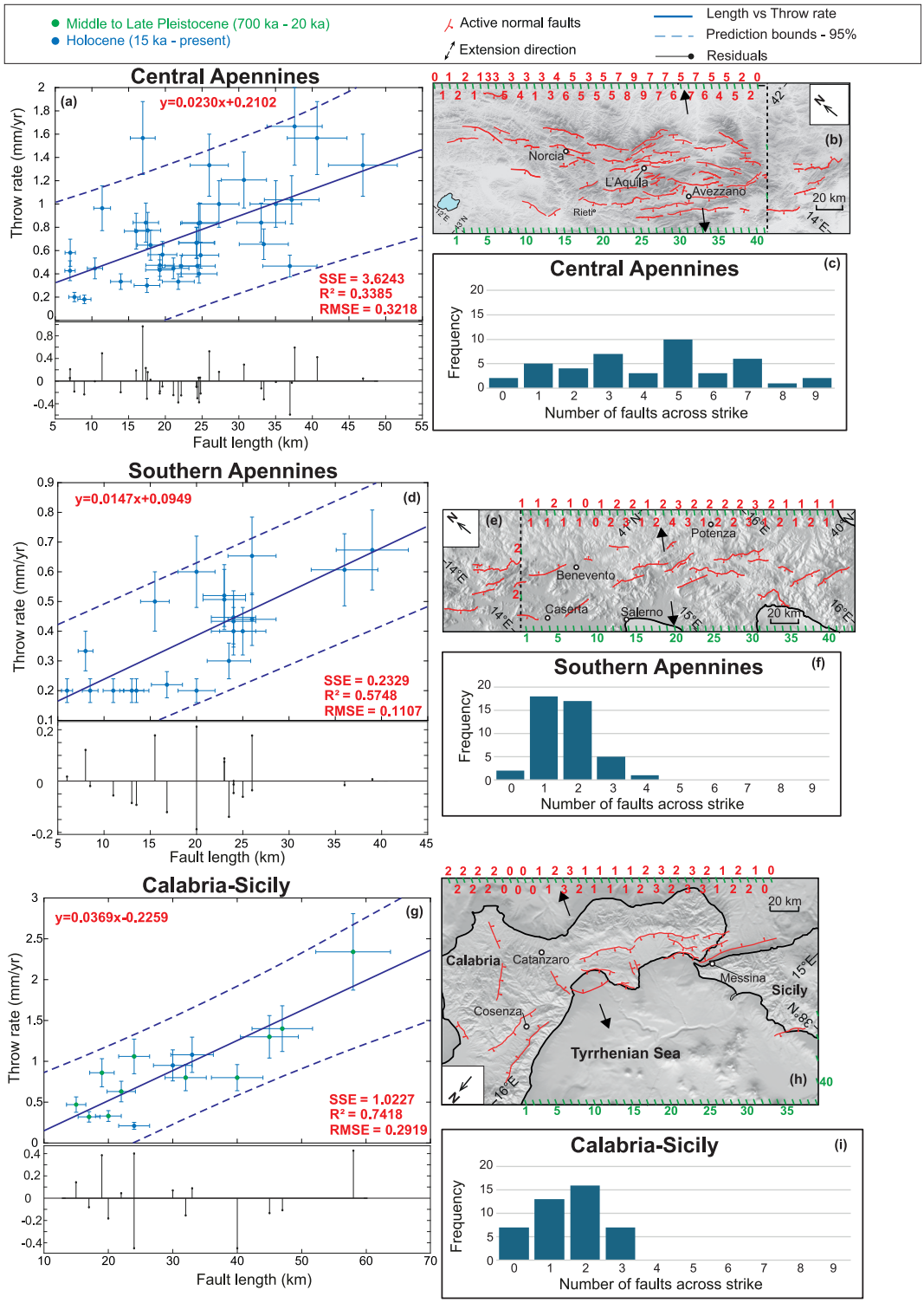

Figure 3. Scaling relationships for throw-rate and fault length for three regions of extensional faulting in Italy compared to other regions. (a)–(c) Show this scaling, and the related residuals, for central Apennines alongside a map of the fault geometries and a histogram of the numbers of fault across strike along the serial transects shown in the maps. (d)–(f) Show this scaling, and the related residuals, for southern Apennines alongside a map of the fault geometries and a histogram of the numbers of fault across strike along the serial transects shown in the maps. (g)–(i) Show this scaling, and the related residuals, for the Calabria-Sicily region alongside a map of the fault geometries and a histogram of the numbers of fault across strike along the serial transects shown in the maps. Note that red-colored numbers are the number of active fault across-strike a transect, which is green-colored.

Table 2
Linear Regression Parameters and Goodness-of-Fit Statistics for the Relationship Between Fault Length and Throw Rate ($y = a{\cdot}length + b$) for Each Study Region and for the Combined Data Set ("All Faults")

	a (lower bound; upper bound)	b (lower and upper bound)	SSE	R^2	RMSE
Calabria and Sicily	0.0369 (0.0232; 0.0506)	−0.2259 (−0.6758; 0.2239)	1.0227	0.7418	0.2919
Southern Apennines	0.0147 (0.0086; 0.0207)	0.0949 (−0.0379; 0.2276)	0.2329	0.5748	0.1107
Central Apennines	0.0230 (0.0120; 0.0340)	0.2102 (−0.0645; 0.4849)	3.6243	0.3385	0.3218
All faults	0.0291 (0.0224; 0.0359)	−0.0476 (−0.227; 0.1275)	6.4770	0.4816	0.3042

Note. Reported values include regression coefficients (a, b), their 95% confidence bounds, the sum of squared errors (SSE), the coefficient of determination (R^2), and the root mean square error (RMSE). SSE reflects the cumulative misfit within each data set and depends on the number of observations, whereas R^2 and RMSE provide measures of correlation strength and scatter that can be compared across data sets.

(parameter "a" in $TR = aL + b$; Table 2) also varies systematically between regions, still showing a residual plot (Figure 3) with an overall symmetric distribution of errors across the entire range fault lengths. Calabria-Sicily yields the steepest gradient, indicating that throw rates are more than twice as sensitive to changes in fault length compared to the Southern Apennines and, approximately 1.5 more times more sensitive than in the Central Apennines. This likely suggest that for a given increment in fault length, the expected increase in throw rate is substantially larger in Calabria-Sicily region than elsewhere along the entire Italian Apennines Chain. We also tentatively suggest that this may reflect the greater maturity and mechanical coherence of the Calabria-Sicily fault system, where fewer across-strike active faults influence the strain portioning among individual faults. However, further analysis of the controls on regression gradients are beyond the scope of this study and more future investigations are needed.

Our data sets in Table 1 and Figure 3 also differ in the geometry of the associated fault systems. The analysis focuses on active faults capable of producing surface-rupturing earthquakes. In the Central Apennines, up to nine active faults are mapped across strike, with an approximately uniform distribution between one and nine across-strike faults (Figures 3b and 3c). In contrast, the Southern Apennines are characterized by a maximum of four across-strike faults, while the Calabria–Sicily region includes no more than three across-strike faults (Figures 3e and 3f for Southern Apennines and Figures 3h and 3i for Calabria-Sicily).

When scatter metrics derived from the regressions (R^2, RMSE, and SSE) are compared with the number of across-strike faults, a consistent pattern emerges (Figure 4). In particular, Figure 4a shows a single combined plot for all 68 faults along the Italian Apennines Chain, the best-fit regression line and 95% confidence bounds. When the entire data set is gathered, the overall correlation between throw rate and fault length is positive even if it shows considerable scatter (R^2 of 0.48 and RMSE of 0.30). This likely reflects the diversity of fault network geometries shown in this study, and confirms that a single regression line is not enough to capture the regional variability documented in Figure 3. Furthermore, data from the Central Apennines define the lower-gradient, higher-scatter portion of the plot, while data from Calabria-Sicily align along preferentially a steeper, tighter trend, visually reinforcing the regional changes mentioned above (Figure 4a). Figure 4b shows R^2 values for the three individual regions in this study as a function of the maximum number of across-strike fault recorded in serial transects (Figures 3b, 3e, and 3h), parallel to the extension direction, alongside the corresponding fault count histograms. This graph tentatively tests our central hypothesis that scatter, as quantified inversely by R^2 value, increases with the number of across-strike faults. Indeed, higher R^2 values are found from Calabria-Sicily where a fewest across-strike faults are recorded ($R^2 = 0.72$), and consistent decrease through the Southern Apennines ($R^2 = 0.55$), to the Central Apennines where highest fault count is recorded ($R^2 = 0.34$). These results support the interpretation that fault network geometry, and specifically across-strike fault density, exerts a first-order control on the scatter of throw-rate versus fault length correlation. This is observed regardless of the statistical metric used to quantify scatter and forms the basis for the interpretation discussed in the following section.

5. Discussion

The relationship between fault displacement and fault length has long been interpreted through the lens of self-similar fault growth. Early mechanical models demonstrated that displacement and length may scale

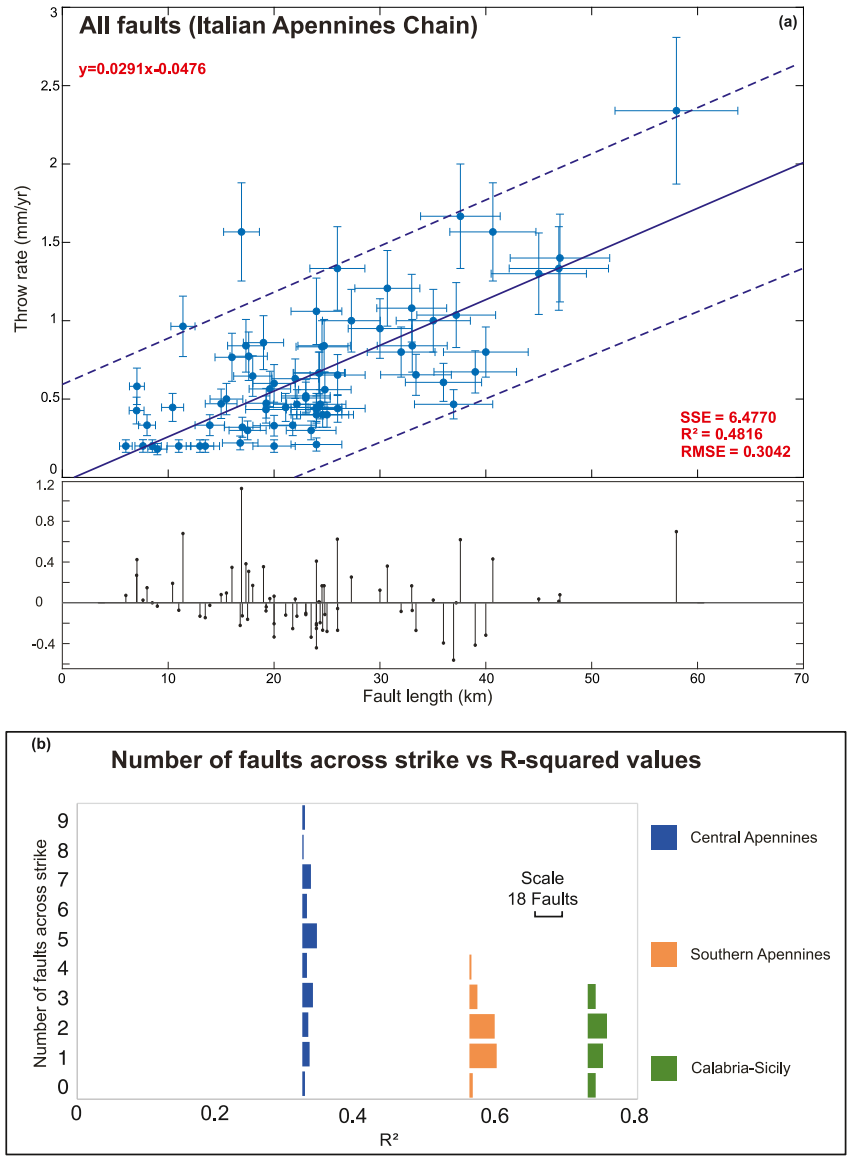

Figure 4. (a) Linear regression between fault length and throw rate for the complete data set of active faults along the Italian Apennines chain ("All faults"), with best-fit line and 95% confidence bounds; residuals are shown in the lower panel. Regression statistics are reported in the inset. (b) Shows the relationships between R^2 values quantifying the scatter in throw-rate versus fault length scaling for each of the three areas, alongside histograms of the numbers of faults across strike within the interaction zone.

proportionally during specific stages of fault evolution, particularly when faults propagate within mechanically homogeneous media and accumulate slip in a self-similar manner (Cowie & Scholz, 1992). However, subsequent compilations of natural data sets have shown that this behavior is not universal. Variability in lithology, mechanical layering, fault maturity, and the degree of segment linkage produces substantial scatter in global data sets, challenging the notion of a single linear scaling law applicable across tectonic settings (Lathrop et al., 2022).

More recent regionally focused studies provide important nuance to this debate. Indeed, when sampling is restricted to fault systems that share comparable mechanical conditions, such as similar maturity, rheology, and tectonic history, linear scaling can re-emerge as a robust descriptor of fault growth. For example, it has been documented a clear linear trend across several orders of magnitude within the mechanically coherent Atacama Fault System, demonstrating that self-similar growth processes can dominate when structural and lithological variability is minimized (Stanton-Yonge et al., 2020). These findings support the view that linear regressions are

appropriate in regionally constrained analyses, whereas broader, heterogeneous data sets require more flexible or non-linear scaling formulations. These differences could be the basis of the different parameterizations of the linear regressions calculated by dividing the data set on a geographical basis. However, this would be beyond the scope of this investigation.

We also highlight that uncertainties in fault length measurements, fault linkage process and throw-rates estimations may surely contribute to scatter the empirical correlations in this study. However, these uncertainties are common to all regions investigated here and cannot explain the systematic differences observed between the three regions. In particular, uncertainty related to soft linkage would be expected to be greatest in densely faulted regions, such as the Central Apennines, and would tend to increase scatter, making the observed reduction in scatter for regions with fewer across-strike faults a conservative result. Nonetheless, independent evidence further supports the robustness of this interpretation. For instance, Faure Walker et al. (2021), using the Fault2SHA Central Apennines database, show that the correlation between fault length and throw rate remains moderate ($R^2 \approx 0.4$; their Figures 4c and 4d). This value is mostly comparable to our correlation obtained in this study ($R^2 \approx 0.34$), suggesting that measurement uncertainty alone does not control the observed scatter. Instead, we suggest that the variability is best explained by differences in fault interaction associated with across-strike fault density.

Our results in Figure 3 suggest that differences in scatter between regions are robust and not dependent on a single measure of goodness of fit and confirm fault length as a first-order control while highlighting additional sources of variability.

Moreover, our results are consistent with the suggestion by Mouslopoulou et al. (2009) that "Stable long-term displacement rates and fluctuations in earthquake recurrence intervals and slip arise, in part, due to fault interactions." We suggest that where the separation of faults across strike is small relative to the distance across-strike, significant stress interactions can occur, and this results in fault slip-rate variability (Figure 2). This is consistent with Sgambato et al. (2023), who show the importance of fault system geometry for controlling the relative importance of coseismic and interseismic stress and in turn overall stress evolution on faults and earthquake occurrence variability.

We have linked our results to measurements of the durations of temporal earthquake clusters, for example, where throw-rates within 42 studied temporal earthquake clusters that occurred in the area we study, lasted on average between 2.83 and 4.26 kyrs, displaying a throw-rate greater than the throw-rate measured over 20 kyrs by mean factor of 6.24 (Roberts et al., 2025). This may go some way toward confirming the suggestion by Mouslopoulou et al. (2009) that scatter in scaling between throw-rates and fault lengths is due to fault interaction. We are able to make this observation because we use throw-rate measurements over longer time periods (20 ka) as opposed to the shorter timescales that are reported to characterize temporal earthquake clustering (2.83–4.26 kyrs; Roberts et al., 2025).

In order to examine our regional results within a broader global framework, we try to compare our data sets with a more global compilation of throw-rates versus fault length presented by Mouslopoulou et al. (2009). In particular, we pursue two main objectives where firstly we assess whether data from the Italian Apennines Chain reproduce the scatter levels reported in a global data set derived from different tectonic settings; secondly, we evaluate whether regionally constrained data sets, such as ours, show reduced scatter compared to heterogenous global ones, consistent with the hypothesis that tectonic setting and fault geometry are key controls. We here recall that for having a better visualization of comparing between our results and those by Mouslopoulou et al. (2009), we have normalized our throw rates and fault lengths following the approach proposed by Mouslopoulou et al. (2009), scaling to a reference fault length of 100 km (see Methods for more details). Figure 5a shows our three normalized regional data sets while Figure 5b shows the Mouslopoulou et al. (2009) compilation. It is interesting to note that our normalized data sets display less scatter overall than the global compilation, which suggests the idea that regional fault arrays sharing comparable mechanical conditions may likely produce more coherent scaling behavior. Furthermore, scatter within our data set is less for regions that have fewer faults across strike (Southern Apennines and Calabria-Sicily) (Figure 4d), compared to the Central Apennines, a zone known to be prone to stress interactions (Figure 2; Mildon, Roberts, Faure Walker, Beck, et al., 2019; Mildon, Roberts, Faure Walker, & Toda, 2019; Sgambato et al., 2023; Sgambato, Faure Walker, Mildon, & Roberts, 2020; G. Valentini et al., 2024; Wedmore et al., 2017). We suggest that, if the regional extension rate is maintained and each across-strike fault contributes to accommodating this extension, an increase in the number of across-strike

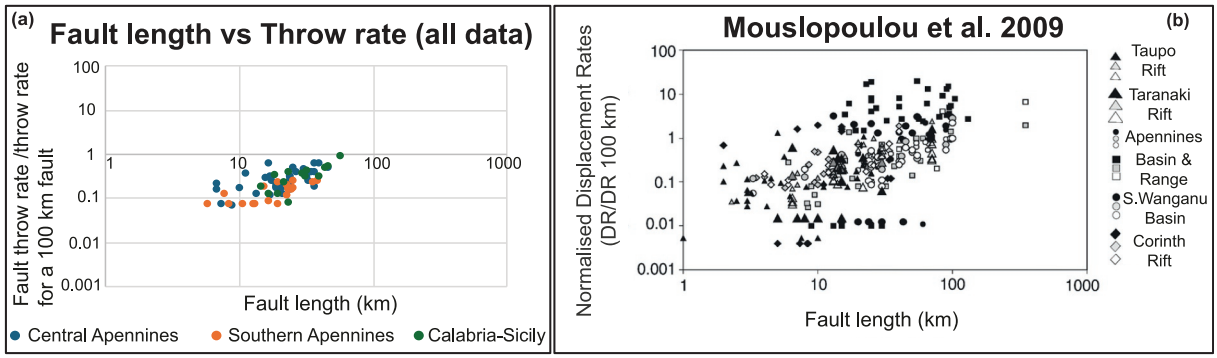

Figure 5. (a) Compilation of all data normalized for the three areas to facilitate comparison with (b). (b) Comparison of throw-rate versus fault length scaling for other regions of extension from Mouslopoulou et al. (2009).

faults promotes greater scatter in throw-rate versus fault-length scaling. This occurs because individual faults participate in temporal clusters characterized by slip/throw rates that exceed long-term averages measured over ~20 kyr. This has important implications for seismic hazard assessment. In many fault systems, the slip or throw rates of individual faults are not well constrained, which limits our ability to estimate recurrence intervals for damaging earthquakes and to characterize the intercepts of frequency–magnitude distributions for specific faults (e.g., Pace et al., 2016; Roberts et al., 2025; Sgambato et al., 2025). However, given knowledge of robust scaling between throw-rate and fault lengths, in the absence of significant scatter, this would facilitate our ability to allocate portions of the regional extension rate to individual faults (e.g., Carafa et al., 2020; Ferranti et al., 2014; Johnson et al., 2020; Meschis, Teza, et al., 2022; Serpelloni et al., 2010; Zeng & Shen, 2016). More specifically, our results suggest that predictive utility of empirical scaling relationships such as ours from this study is strongly dependent on fault network geometry. Indeed, in regions characterized by simple fault arrays with a few active faults across-strike, like our Calabria-Sicily data set, scaling relationships may provide reasonable reliable first-order estimates of throw rate from measured and properly mapped fault length. These estimates might influence seismic hazard assessments where throw rate data are lacking. In contrast, regions characterized by fault arrays that are geometrically more complex, with multiple closely spaced across-strike interacting faults, scaling relationships are expected to carry significant uncertainties and should be applied more cautiously. Our results suggest that the endeavor of allocating portions of the regional extension rate to individual faults using scaling relationships between throw-rate and fault length, should include consideration of fault dimensions, geometric moment, and the numbers of faults across strike within the interaction zone. This same is true for calculations of rheological properties of the continental crust in extension, such as viscosity of the viscous shear zones in the middle and lower crust, using slip or throw rate data and the localized or distributed nature of the active fault system (Cowie et al., 2005; England & Molnar, 1997; Roberts et al., 2025).

6. Conclusions

We present a regional analysis of throw-rate versus fault-length scaling in three extensional domains of the Italian Apennines Chain characterized by progressively increasing numbers of active faults across strike. Using multiple statistical measures (R^2, RMSE, and SSE), we show that the strength of the scaling relationship decreases and scatter increases in regions where a greater number of faults interact across strike. This pattern is robust to uncertainties in fault length definition and to slip/throw-rate estimates averaged over Holocene to Late Quaternary timescales, which are sufficiently long to smooth short-term temporal clustering. Our results indicate that fault interaction exerts a first-order control on the variability of fault slip/throw rates and should be explicitly taken into account when applying empirical scaling relationships to seismic hazard assessment and to models of strain partitioning and crustal rheology in continental extensional settings.

Conflict of Interest

The authors declare no conflicts of interest relevant to this study.

Availability Statement

All data necessary to reproduce the results presented in this study (fault lengths and throw rates) are compiled in Table 1 of the manuscript. Therefore, no additional external repository is required.

Acknowledgments
This work was supported by an INGV-led project (*Idro1.RM task 1 9999.710 CR 7101—Rete multiparametrica*). Z. Mildon was supported by UKRI Future Leaders Fellowship [Grant MR/T041994/1]. G.P. Roberts and J.P. Faure Walker were supported by grants NERC Standard Grant NE/V012894/1; G.P. Roberts was supported by NERC Standard Grant NE/I024127/1; NERC Large Grant. NE/J016497/1; NERC Studentship NE/L002485/1. We finally gratefully acknowledge the Associate Editor, Prof. Rebecca Bell, and the reviewers, Dr. Alex Whittaker and one anonymous reviewer, for their insightful and constructive comments, which have significantly improved the quality of this manuscript. Open access publishing facilitated by Istituto Nazionale di Geofisica e Vulcanologia, as part of the Wiley - CRUI-CARE agreement.

References

Aloisi, M., Bruno, V., Cannavò, F., Ferranti, L., Mattia, M., Monaco, C., & Palano, M. (2013). Are the source models of the M 7.1 1908 Messina Straits earthquake reliable? Insights from a novel inversion and a sensitivity analysis of levelling data. *Geophysical Journal International*, *192*(3), 1025–1041. https://doi.org/10.1093/gji/ggs062

Anderson, J. G., Biasi, G. P., Angster, S., & Wesnousky, S. G. (2021). Improved scaling relationships for seismic moment and average slip of strike-slip earthquakes incorporating fault-slip rate, fault width, and stress drop. *Bulletin of the Seismological Society of America*, *111*(5), 2379–2392. https://doi.org/10.1785/0120210113

Carafa, M. M. C., Galvani, A., Di Naccio, D., Kastelic, V., Di Lorenzo, C., Miccolis, S., et al. (2020). Partitioning the ongoing extension of the Central Apennines (Italy): Fault slip rates and bulk deformation rates from geodetic and stress data. *Journal of Geophysical Research: Solid Earth*, *125*(7), e2019JB018956. https://doi.org/10.1029/2019JB018956

Carminati, E., Lustrino, M., Cuffaro, M., & Doglioni, C. (2010). Tectonics, magmatism and geodynamics of Italy: What we know and what we imagine. *Journal of the Virtual Explorer*, *36*. https://doi.org/10.3809/jvirtex.2010.00226

Cavinato, G. P., & Celles, P. G. D. (1999). Extensional basins in the tectonically bimodal central Apennines fold-thrust belt, Italy: Response to corner flow above a subducting slab in retrograde motion. *Geology*, *27*(10), 955. https://doi.org/10.1130/0091-7613(1999)027<0955:EBITTB>2.3.CO;2

Cowie, P. A., & Roberts, G. P. (2001). Constraining slip rates and spacings for active normal faults. *Journal of Structural Geology*, *23*(12), 1901–1915. https://doi.org/10.1016/S0191-8141(01)00036-0

Cowie, P. A., Roberts, G. P., Bull, J. M., & Visini, F. (2012). Relationships between fault geometry, slip rate variability and earthquake recurrence in extensional settings. *Geophysical Journal International*, *189*(1), 143–160. https://doi.org/10.1111/j.1365-246X.2012.05378.x

Cowie, P. A., & Scholz, C. H. (1992). Displacement-length scaling relationship for faults: Data synthesis and discussion. *Journal of Structural Geology*, *14*(10), 1149–1156. https://doi.org/10.1016/0191-8141(92)90066-6

Cowie, P. A., Underhill, J., Behn, M., Lin, J., & Gill, C. (2005). Spatio-temporal evolution of strain accumulation derived from multi-scale observations of Late Jurassic rifting in the northern North Sea: A critical test of models for lithospheric extension. *Earth and Planetary Science Letters*, *234*(3–4), 401–419. https://doi.org/10.1016/j.epsl.2005.01.039

D'Agostino, N., Jackson, J. A., Dramis, F., & Funiciello, R. (2001). Interactions between mantle upwelling, drainage evolution and active normal faulting: An example from the central Apennines (Italy). *Geophysical Journal International*, *147*(2), 475–497. https://doi.org/10.1046/j.1365-246X.2001.00539.x

Devoti, R., Esposito, A., Pietrantonio, G., Pisani, A. R., & Riguzzi, F. (2011). Evidence of large scale deformation patterns from GPS data in the Italian subduction boundary. *Earth and Planetary Science Letters*, *311*(3–4), 230–241. https://doi.org/10.1016/j.epsl.2011.09.034

Doglioni, C. (1993). Some remarks on the origin of foredeeps. *Tectonophysics*, *228*(1–2), 1–20. https://doi.org/10.1016/0040-1951(93)90211-2

England, P., & Molnar, P. (1997). Active deformation of Asia: From kinematics to dynamics. *Science*, *278*(5338), 647–650. https://doi.org/10.1126/science.278.5338.647

Faccenna, C., Funiciello, F., Giardini, D., & Lucente, P. (2001). Episodic back-arc extension during restricted mantle convection in the Central Mediterranean. *Earth and Planetary Science Letters*, *187*(1–2), 105–116. https://doi.org/10.1016/S0012-821X(01)00280-1

Faure Walker, J. P., Boncio, P., Pace, B., Roberts, G. P., Benedetti, L., Scotti, O., et al. (2021). Fault2SHA Central Apennines database and structuring active fault data for seismic hazard assessment. *Scientific Data*, *8*(87), 1–20. https://doi.org/10.1038/s41597-021-00868-0

Faure Walker, J. P., Roberts, G. P., Cowie, P. A., Papanikolaou, I., Michetti, A. M., Sammonds, P., et al. (2012). Relationship between topography, rates of extension and mantle dynamics in the actively-extending Italian Apennines. *Earth and Planetary Science Letters*, *325–326*, 76–84. https://doi.org/10.1016/j.epsl.2012.01.028

Faure Walker, J. P., Roberts, G. P., Cowie, P. A., Papanikolaou, I. D., Sammonds, P. R., Michetti, A. M., & Phillips, R. J. (2009). Horizontal strain-rates and throw-rates across breached relay zones, central Italy: Implications for the preservation of throw deficits at points of normal fault linkage. *Journal of Structural Geology*, *31*(10), 1145–1160. https://doi.org/10.1016/j.jsg.2009.06.011

Ferranti, L., Antonioli, F., Mauz, B., Amorosi, A., Dai Pra, G., Mastronuzzi, G., et al. (2006). Markers of the last interglacial sea-level high stand along the coast of Italy: Tectonic implications. *Quaternary International*, *145–146*, 30–54. https://doi.org/10.1016/j.quaint.2005.07.009

Ferranti, L., Monaco, C., Antonioli, F., Maschio, L., Kershaw, S., & Verrubbi, V. (2007). The contribution of regional uplift and coseismic slip to the vertical crustal motion in the Messina Straits, southern Italy: Evidence from raised Late Holocene shorelines. *Journal of Geophysical Research*, *112*(B6), B06401. https://doi.org/10.1029/2006JB004473

Ferranti, L., Monaco, C., Morelli, D., Antonioli, F., & Maschio, L. (2008). Holocene activity of the Scilla Fault, Southern Calabria: Insights from coastal morphological and structural investigations. *Tectonophysics*, *453*(1–4), 74–93. https://doi.org/10.1016/j.tecto.2007.05.006

Ferranti, L., Palano, M., Cannavò, F., Mazzella, M. E., Oldow, J. S., Gueguen, E., et al. (2014). Rates of geodetic deformation across active faults in southern Italy. *Tectonophysics*, *621*, 101–122. https://doi.org/10.1016/j.tecto.2014.02.007

Field, E. H., Arrowsmith, R. J., Biasi, G. P., Bird, P., Dawson, T. E., Felzer, K. R., et al. (2014). Uniform California Earthquake Rupture Forecast, Version 3 (UCERF3)—The time-independent model. *Bulletin of the Seismological Society of America*, *104*(3), 1122–1180. https://doi.org/10.1785/0120130164

Galli, P., & Bosi, V. (2003). Catastrophic 1638 earthquakes in Calabria (southern Italy): New insights from paleoseismological investigation. *Journal of Geophysical Research*, *108*(B1), ETG1-1–ETG1-20. https://doi.org/10.1029/2001JB001713

Galli, P., Galadini, F., & Pantosti, D. (2008). Twenty years of paleoseismology in Italy. *Earth-Science Reviews*, *88*(1–2), 89–117. https://doi.org/10.1016/j.earscirev.2008.01.001

Galli, P., Scionti, V., & Spina, V. (2007). New paleoseismic data from the Lakes and Serre faults: Seismotectonic implications for Calabria (Southern Italy). *Bollettino della Societa Geologica Italiana*, *126*(2), 347–364.

Galli, P., Spina, V., Ilardo, I., & Naso, G. (2011). Evidence of active tectonics in southern Italy: The Rossano fault (Calabria). In *Recent Progress on Earthquake Geology*.

Giuffrida, S., Brighenti, F., Cannavò, F., Carnemolla, F., De Guidi, G., Barreca, G., et al. (2023). Multidisciplinary analysis of 3D seismotectonic modelling: A case study of Serre and Cittanova faults in the southern Calabrian Arc (Italy). *Frontiers in Earth Science*, *11*, 1240051. https://doi.org/10.3389/feart.2023.1240051

Gómez-Novell, O., Ortuño, M., García-Mayordomo, J., Insua-Arévalo, J. M., Rockwell, T. K., Baize, S., et al. (2022). Improved geological slip rate estimations in the complex Alhama De Murcia Fault Zone (SE Iberia) and its implications for fault behavior. *Tectonics*, *41*(12), e2022TC007465. https://doi.org/10.1029/2022TC007465

Gupta, A., & Scholz, C. H. (2000). A model of normal fault interaction based on observations and theory. *Journal of Structural Geology*, *22*(7), 865–879. https://doi.org/10.1016/S0191-8141(00)00011-0

Gvirtzman, Z., & Nur, A. (1999). The formation of Mount Etna as the consequence of slab rollback. *Nature*, *401*, 782–785. https://doi.org/10.1038/44555

Gvirtzman, Z., & Nur, A. (2001). Residual topography, lithospheric structure and sunken slabs in the central Mediterranean. *Earth and Planetary Science Letters*, *187*(1–2), 117–130. https://doi.org/10.1016/S0012-821X(01)00272-2

Iezzi, F., Roberts, G., Faure Walker, J., Papanikolaou, I., Ganas, A., Deligiannakis, G., et al. (2021). Temporal and spatial earthquake clustering revealed through comparison of millennial strain-rates from 36Cl cosmogenic exposure dating and decadal GPS strain-rate. *Scientific Reports*, *11*(1), 23320. https://doi.org/10.1038/s41598-021-02131-3

Iezzi, F., Roberts, G., Walker, J. F., & Papanikolaou, I. (2019). Occurrence of partial and total coseismic ruptures of segmented normal fault systems: Insights from the Central Apennines, Italy. *Journal of Structural Geology*, *126*, 83–99. https://doi.org/10.1016/j.jsg.2019.05.003

Jacques, E., Monaco, C., Tapponnier, P., Tortorici, L., & Winter, T. (2001). Faulting and earthquake triggering during the 1783 Calabria seismic sequence. *Geophysical Journal International*, *147*(3), 499–516. https://doi.org/10.1046/j.0956-540x.2001.01518.x

Johnson, K. M., Hammond, W. C., Burgette, R. J., Marshall, S. T., & Sorlien, C. C. (2020). Present-day and long-term uplift across the western transverse ranges of Southern California. *Journal of Geophysical Research: Solid Earth*, *125*(8), 1–20. https://doi.org/10.1029/2020JB019672

Lathrop, B. A., Jackson, C. A.-L., Bell, R. E., & Rotevatn, A. (2022). Displacement/length scaling relationships for normal faults; a review, critique, and revised compilation. *Frontiers in Earth Science*, *10*, 907543. https://doi.org/10.3389/feart.2022.907543

Loreto, M. F., Capotondi, L., Insinga, D. D., Molisso, F., Vigliotti, L., Albertazzi, S., et al. (2023). Slip-rates and time recurrences of the seismogenic Sant'Eufemia normal fault (SE Tyrrhenian Sea), a multiscale and multidisciplinary approach. *Marine and Petroleum Geology*, *156*, 106453. https://doi.org/10.1016/j.marpetgeo.2023.106453

Malinverno, A., & Ryan, W. B. F. (1986). Extension in the Tyrrhenian Sea and shortening in the Apennines as result of arc migration driven by sinking of the lithosphere. *Tectonics*, *5*(2), 227–245. https://doi.org/10.1029/TC005i002p00227

Mastrolembo Ventura, B., Serpelloni, E., Argnani, A., Bonforte, A., Bürgmann, R., Anzidei, M., et al. (2014). Fast geodetic strain-rates in eastern Sicily (southern Italy): New insights into block tectonics and seismic potential in the area of the great 1693 earthquake. *Earth and Planetary Science Letters*, *404*, 77–88. https://doi.org/10.1016/j.epsl.2014.07.025

Meschis, M., Roberts, G. P., Mildon, Z. K., Robertson, J., Michetti, A. M., & Faure Walker, J. P. (2019). Slip on a mapped normal fault for the 28th December 1908 Messina earthquake (Mw 7.1) in Italy. *Scientific Reports*, *9*, 1–8. https://doi.org/10.1038/s41598-019-42915-2

Meschis, M., Roberts, G. P., Robertson, J., & Briant, R. M. (2018). The relationships between regional quaternary uplift, deformation across active normal faults, and historical seismicity in the upper plate of subduction zones: The Capo D'Orlando Fault, NE Sicily. *Tectonics*, *37*(5), 1231–1255. https://doi.org/10.1029/2017TC004705

Meschis, M., Roberts, G. P., Robertson, J., Mildon, Z. K., Sahy, D., Goswami, R., et al. (2022). Out of phase Quaternary uplift-rate changes reveal normal fault interaction, implied by deformed marine palaeoshorelines. *Geomorphology*, *416*, 108432. https://doi.org/10.1016/j.geomorph.2022.108432

Meschis, M., Teza, G., Serpelloni, E., Elia, L., Lattanzi, G., Di Donato, M., & Castellaro, S. (2022). Refining rates of active crustal deformation in the upper plate of subduction zones, implied by geological and geodetic data: The e-dipping West Crati Fault, Southern Italy. *Remote Sensing*, *14*(21), 5303. https://doi.org/10.3390/rs14215303

Mildon, Z. K., Roberts, G. P., Faure Walker, J. P., Beck, J., Papanikolaou, I., Michetti, A. M., et al. (2022). Surface faulting earthquake clustering controlled by fault and shear-zone interactions. *Nature Communications*, *13*(1), 7126. https://doi.org/10.1038/s41467-022-34821-5

Mildon, Z. K., Roberts, G. P., Faure Walker, J. P., Beck, J. W., Papanikolaou, I. D., Michetti, A. M., et al. (2019). Earthquake clustering controlled by shear zone interaction. https://doi.org/10.31223/osf.io/qkx2v

Mildon, Z. K., Roberts, G. P., Faure Walker, J. P., & Toda, S. (2019). Coulomb pre-stress and fault bends are ignored yet vital factors for earthquake triggering and hazard. *Nature Communications*, *10*(1), 2744. https://doi.org/10.1038/s41467-019-10520-6

Molnar, P. (1979). Earthquake recurrence intervals and plate tectonics. *Bulletin of the Seismological Society of America*, *69*(1), 115–133. https://doi.org/10.1785/BSSA0690010115

Monaco, C., & Tortorici, L. (2000). Active faulting in the Calabrian arc and eastern Sicily. *Journal of Geodynamics*, *29*(3–5), 407–424. https://doi.org/10.1016/S0264-3707(99)00052-6

Monaco, C., & Tortorici, L. (2007). Active faulting and related tsunamis in eastern Sicily and south-western Calabria. *Bollettino di Geofisica Teorica ed Applicata*, *48*(2), 163–184.

Mouslopoulou, V., Walsh, J. J., & Nicol, A. (2009). Fault displacement rates on a range of timescales. *Earth and Planetary Science Letters*, *278*(3–4), 186–197. https://doi.org/10.1016/j.epsl.2008.11.031

Nicol, A., Walsh, J. J., Manzocchi, T., & Morewood, N. (2005). Displacement rates and average earthquake recurrence intervals on normal faults. *Journal of Structural Geology*, *27*(3), 541–551. https://doi.org/10.1016/j.jsg.2004.10.009

Pace, B., Peruzza, L., Lavecchia, G., & Boncio, P. (2006). Layered seismogenic source model and probabilistic seismic-hazard analyses in Central Italy. *Bulletin of the Seismological Society of America*, *96*(1), 107–132. https://doi.org/10.1785/0120040231

Pace, B., Visini, F., & Peruzza, L. (2016). FiSH: MATLAB tools to turn fault data into seismic-hazard models. *Seismological Research Letters*, *87*(2A), 374–386. https://doi.org/10.1785/0220150189

Papanikolaou, I. D., & Roberts, G. P. (2007). Geometry, kinematics and deformation rates along the active normal fault system in the southern Apennines: Implications for fault growth. *Journal of Structural Geology*, *29*(1), 166–188. https://doi.org/10.1016/j.jsg.2006.07.009

Patacca, E., & Scandone, P. (2007). Geological interpretation of the CROP-04 seismic line (Southern Apennines, Italy).

Peruzza, L., Pace, B., & Visini, F. (2011). Fault-based earthquake rupture forecast in Central Italy: Remarks after the L'Aquila Mw 6.3 event. *Bulletin of the Seismological Society of America*, *101*(1), 404–412. https://doi.org/10.1785/0120090276

Quye-Sawyer, J., Whittaker, A. C., Roberts, G., & Rood, D. (2021). Fault throw and regional uplift histories from drainage analysis: Evolution of Southern Italy. *Tectonics*, *40*(4), e2020TC006076. https://doi.org/10.1029/2020TC006076

Roberts, G. P., Iezzi, F., Sgambato, C., Robertson, J., Beck, J., Mildon, Z. K., et al. (2025). Characteristics and modelling of slip-rate variability and temporal earthquake clustering across a distributed network of active normal faults constrained by in situ ^{36}Cl cosmogenic dating of fault scarp exhumation, central Italy. *Journal of Structural Geology*, *195*, 105391. https://doi.org/10.1016/j.jsg.2025.105391

Roberts, G. P., Meschis, M., Houghton, S., Underwood, C., & Briant, R. M. (2013). The implications of revised Quaternary palaeoshoreline chronologies for the rates of active extension and uplift in the upper plate of subduction zones. *Quaternary Science Reviews*, *78*, 169–187. https://doi.org/10.1016/j.quascirev.2013.08.006

Roberts, G. P., & Michetti, A. M. (2004). Spatial and temporal variations in growth rates along active normal fault systems: An example from The Lazio–Abruzzo Apennines, central Italy. *Journal of Structural Geology*, *26*(2), 339–376. https://doi.org/10.1016/S0191-8141(03)00103-2

Roberts, G. P., Sgambato, C., Mildon, Z. K., Iezzi, F., Beck, J., Robertson, J., et al. (2024). Spatial migration of temporal earthquake clusters driven by the transfer of differential stress between neighbouring fault/shear-zone structures. *Journal of Structural Geology*, *181*, 105096. https://doi.org/10.1016/j.jsg.2024.105096

Roda-Boluda, D. C., & Whittaker, A. C. (2017). Structural and geomorphological constraints on active normal faulting and landscape evolution in Calabria, Italy. *Journal of the Geological Society*, *174*(4), jgs2016-097. https://doi.org/10.1144/jgs2016-097

Rodriguez Piceda, C., Mildon, Z. K., Van Den Ende, M., Ampuero, J., & Andrews, B. J. (2025). Normal fault interactions in seismic cycles and the impact of fault network geometry. *Journal of Geophysical Research: Solid Earth*, *130*(4), e2024JB030382. https://doi.org/10.1029/2024JB030382

Rotevatn, A., Jackson, C. A. L., Tvedt, A. B. M., Bell, R. E., & Blækkan, I. (2019). How do normal faults grow? *Journal of Structural Geology*, *125*, 174–184. https://doi.org/10.1016/j.jsg.2018.08.005

Schirripa Spagnolo, G., Mercuri, M., Billi, A., Carminati, E., & Galli, P. (2021). The segmented campo Felice Normal Faults: Seismic potential appraisal by application of empirical relationships between rupture length and earthquake magnitude in the Central Apennines, Italy. *Tectonics*, *40*(7), e2020TC006465. https://doi.org/10.1029/2020TC006465

Scholz, C. H., & Cowie, P. A. (1990). Determination of total strain from faulting using slip measurements. *Nature*, *346*(6287), 837–839. https://doi.org/10.1038/346837a0

Serpelloni, E., Anzidei, M., Baldi, P., Casula, G., & Galvani, A. (2005). Crustal velocity and strain-rate fields in Italy and surrounding regions: New results from the analysis of permanent and non-permanent GPS networks. *Geophysical Journal International*, *161*(3), 861–880. https://doi.org/10.1111/j.1365-246X.2005.02618.x

Serpelloni, E., Bürgmann, R., Anzidei, M., Baldi, P., Mastrolembo Ventura, B., & Boschi, E. (2010). Strain accumulation across the Messina Straits and kinematics of Sicily and Calabria from GPS data and dislocation modeling. *Earth and Planetary Science Letters*, *298*(3–4), 347–360. https://doi.org/10.1016/j.epsl.2010.08.005

Sgambato, C., Faure Walker, J. P., Mildon, Z. K., & Roberts, G. P. (2020). Stress loading history of earthquake faults influenced by fault/shear zone geometry and Coulomb pre-stress. *Scientific Reports*, *10*(1), 12724. https://doi.org/10.1038/s41598-020-69681-w

Sgambato, C., Faure Walker, J. P., & Roberts, G. P. (2020). Uncertainty in strain-rate from field measurements of the geometry, rates and kinematics of active normal faults: Implications for seismic hazard assessment. *Journal of Structural Geology*, *131*, 103934. https://doi.org/10.1016/j.jsg.2019.103934

Sgambato, C., Faure Walker, J. P., Roberts, G. P., Mildon, Z. K., & Meschis, M. (2023). Influence of fault system geometry and slip rates on the relative role of coseismic and interseismic stresses on earthquake triggering and recurrence variability. *Journal of Geophysical Research: Solid Earth*, *128*(11), e2023JB026496. https://doi.org/10.1029/2023JB026496

Sgambato, C., Roberts, G. P., Iezzi, F., Faure Walker, J. P., Beck, J., Mildon, Z. K., et al. (2025). Millennial slip-rates variability of along-strike active faults in the Italian Southern Apennines Revealed by Cosmogenic ^{36}Cl Dating of Fault Scarps. *Tectonics*, *44*(3), e2024TC008529. https://doi.org/10.1029/2024TC008529

Stanton-Yonge, A., Cembrano, J., Griffith, W. A., Jensen, E., & Mitchell, T. M. (2020). Self-similar length-displacement scaling achieved by scale-dependent growth processes: Evidence from the Atacama Fault System. *Journal of Structural Geology*, *133*, 103993. https://doi.org/10.1016/j.jsg.2020.103993

Tortorici, L., Monaco, C., Tansi, C., & Cocina, O. (1995). Recent and active tectonics in the Calabrian arc (Southern Italy). *Tectonophysics*, *243*(1–2), 37–55. https://doi.org/10.1016/0040-1951(94)00190-K

Valentini, A., Visini, F., & Pace, B. (2017). Integrating faults and past earthquakes into a probabilistic seismic hazard model for peninsular Italy. *Natural Hazards and Earth System Sciences*, *17*(11), 2017–2039. https://doi.org/10.5194/nhess-17-2017-2017

Valentini, G., Volatili, T., Galli, P., & Tondi, E. (2024). Investigating the Last Millennium Coulomb Stress Transfer in the Central Apennine Fault System (CAFS). *Tectonics*, *43*(10), e2024TC008328. https://doi.org/10.1029/2024TC008328

Walker, F. (2010). *Mechanics of continental extension from Quaternary strain fields in the Italian Apennines*. UCL (University College London).

Wedmore, L. N. J., Faure Walker, J. P., Roberts, G. P., Sammonds, P. R., McCaffrey, K. J. W., & Cowie, P. A. (2017). A 667 year record of coseismic and interseismic Coulomb stress changes in central Italy reveals the role of fault interaction in controlling irregular earthquake recurrence intervals. *Journal of Geophysical Research: Solid Earth*, *122*(7), 5691–5711. https://doi.org/10.1002/2017JB014054

Wells, D. L., & Coppersmith, K. J. (1994). New empirical relationships among magnitude, rupture length, rupture width, rupture area, and surface displacement. *Bulletin of the Seismological Society of America*, *84*(4), 974–1002. https://doi.org/10.1785/bssa0840040974

Wesnousky, S. G. (1999). Crustal deformation processes and the stability of the Gutenberg-Richter relationship. *Bulletin of the Seismological Society of America*, *89*(4), 1131–1137. https://doi.org/10.1785/bssa0890041131

Wesnousky, S. G. (2008). Displacement and geometrical characteristics of earthquake surface ruptures: Issues and implications for seismic-hazard analysis and the process of earthquake rupture. *Bulletin of the Seismological Society of America*, *98*(4), 1609–1632. https://doi.org/10.1785/0120070111

Westaway, R. (1993). Quaternary uplift of southern Italy. *Journal of Geophysical Research*, *98*(B12), 741–772. https://doi.org/10.1029/93JB01566

Zeng, Y., & Shen, Z. (2016). A fault-based model for crustal deformation, fault slip rates, and off-fault strain rate in California. *Bulletin of the Seismological Society of America*, *106*(2), 766–784. https://doi.org/10.1785/0120140250